

ELECTROCHEMICAL PROPERTIES OF ALKALINE EARTH METALS-DOPED LANTHANUM MANGANITES FOR SOFC APPLICATIONS

E.Magnone¹, L.Folco¹, A.Martinelli² and M.Ferretti^{1,2}

¹ Dipartimento di Chimica e Chimica Industriale, Università di Genova, Via Dodecaneso 31, I-16146, Genova, Italy

² LAMIA-INFN, Corso Perrone 24, I-16152, Genova, Italy

Electrochemical ac impedance spectroscopy methods were used to study the oxygen reaction kinetics of $\text{La}_x\text{Ca}_{1-x}\text{MnO}_3$ -based cathodes on Y_2O_3 -stabilized ZrO_2 ($0 < x < 1$). The manganite samples have been prepared by conventional solid state reaction using stoichiometric amounts of the precursor oxides. All samples have been characterised by XRD analysis and scanning electron microscope equipped with energy dispersive spectrometer. The impedance spectroscopy measurements were carried out as a function of temperature and phase composition; ten compositions were studied at temperatures between $\sim 900\text{K}$ and $\sim 1273\text{K}$.

The aim of the investigation is to determine the Activation Energy (E_{el}) as a function of electrode compositions (x) for alkaline earth metal-doped lanthanum manganite perovskite electrodes and to identify the mechanism of the oxygen reduction process; in general, the objective of this work is to enable to successfully apply electrochemical impedance techniques to our application needs.

First experimental results were interpreted in the form of equivalent electrical circuit fitting, and compared with the results reported in the literature. A minimum of two overlapping arcs can be distinguished in the impedance spectra at low temperature ($T < 800\text{K}$) while an arc whose resistance R_{el} (determined by activation energy in according to the Arrhenius equations) with a high activation energy was observed for the perovskite-type oxide electrodes at high temperature ($T > 973\text{K}$).

Keywords: Powders-solid state reaction, interfaces, impedance, perovskites, fuel cells.

Introductions

Perovskite-type oxides like LnMO_3 (Ln is a rare-earth element and M is Cr, Mn, Fe, Co or Ni) are expected to be potential catalytic materials for technologically important process. In fact, perovskite-related oxides are of great interest as materials for solid oxide fuel cell (SOFC), oxygen separation membranes, membrane reactors for hydrocarbon partial oxidation, solid electrolyte pumps and sensors. The properties of such oxides, determined by cations occupation of the A and B sites of the ABO_3 perovskite crystal lattice as well as external conditions such as temperature and oxygen partial pressure, vary over a wide range and can be controlled by a partial substitution in both cation sublattices¹.

Alkaline earth metal-doped lanthanum manganite perovskite $\text{La}_x\text{A}_{1-x}\text{MnO}_3$ (with A= Sr, Ca, Ba and $0 < x < 1$) is regarded as one of the most promising cathode materials for use in the production SOCFs because of its high thermal and chemical stability, relatively good compatibility with yttria-stabilized zirconia (YSZ), good electrical conductivity and its low overpotential².

The properties (crystal structure, magnetic properties, electrical conductivity, activation energy, etc) of the La-deficient manganites, $\text{La}_x\text{Ca}_{1-x}\text{MnO}_3$, widely depend on the preparation conditions, which determine the defect concentrations in the cation and anion sublattices³. For example, quenching $\text{La}_x\text{Ca}_{1-x}\text{MnO}_3$ ceramics after annealing in air at 1720 K usually leads to decreased conductivity and an increase in activation energy for electrical conductivity compared to the specimens cooled slowly⁴ but, at the same time, in the superdoped $\text{La}_x\text{Ca}_{1-x}\text{MnO}_3$ compounds (with $x > 0.7$) prepared under conventional conditions, Mn^{4+} proportion is reported to be almost independent of doping level⁵. In addition doping lanthanum perovskite oxides with alkaline earth metal was demonstrated to increase the sinterability of the ceramics⁶. On the other hand, one should

note that both the electrical conductivity, activation energy, and thermal expansion of manganites are functions of pre-history of the ceramics.

For calcium-substituted lanthanum manganites the phase composition could be even more complex^{7,8} and consequently the electrochemical performance of $\text{La}_x\text{Ca}_{1-x}\text{MnO}_3$ -YSZ cathodes is very sensitive to composition^{9,10}.

The performance of SOFCs is often limited by the oxygen transfer process at the cathode¹¹. This is especially true in recently developed thin-electrolyte SOFCs, where the YSZ electrolyte resistance is negligible down to 950 K^{12,13}. Impedance spectroscopy is useful to characterise the kinetics of the $\text{La}_{1-x}\text{Sr}_x\text{MnO}_3$ /YSZ interface¹⁴. Several experimental factors related to the composition are of great importance for the properties of the cathode and thus for performance of SOFCs^{15,16,17}. Accordingly, the diagram shape depends on the electrode morphology and can be composed of one or two more or less overlapping semicircle¹⁸.

Thus, in the present study, the aim is to clarify the relationship between the phase composition and electrochemical impedance spectroscopy measurements of $\text{La}_x\text{Ca}_{1-x}\text{MnO}_3$ (with $0 < x < 1$)–based electrodes on Y_2O_3 -stabilized ZrO_2 . The present study brings another view to this frame, with the help of electrochemical *ac* impedance spectroscopy methods to systematically investigate the oxygen transfer process at the perovskite cathode.

Experimental

Eight mol% Y_2O_3 stabilized ZrO_2 (YSZ, Frialit - Degussit) was used as the electrolyte. $\text{La}_x\text{Ca}_{1-x}\text{MnO}_3$ ($0 < x < 1$) manganite were prepared by conventional solid state reaction at 1623 K using stoichiometric amounts of the high purity precursor oxides La_2O_3 , CaO and MnO_2 . Precursor powders were carefully mixed in a common ball milling in agate jars under ethanol (96%) for approximately 1 h. After drying, the mixture was placed in an Al_2O_3 crucible and put into hot furnace in air, at the synthesis temperature. All samples have been characterised structurally by XRD powder diffractometer (Cu $K\alpha$ radiation, Ni filter).

The cathodic performance was analysed with a three-electrode configuration. A screen printing technique was used to apply the electrode to the electrolyte pellets (YSZ). The electrode was sintered at 1373 K for 1 h. All the working electrodes had an area of about 0.322 cm²; the effect of the electrode thickness was not investigated in this work¹⁹.

A Pt reference electrode was painted with the 6926 Engelhard Pt on the same side as the working electrode, and care was taken to leave a distance as large as possible between the reference and working electrodes in order to prevent systematic errors in the measurement of the impedance characteristic. For the counter-electrode, Pt paste was painted on the other side of the pellet. From a geometrical point of view, the La_xCa_{1-x}MnO₃/YSZ electrodes were arranged on the circular surfaces of the solid electrolyte in order to achieve experimental conditions based on cylindrical symmetry²⁰.

A Solartron electrochemical system (SI1287 Electrochemical Interface and 1260 Impedance/Gain-Phase Analyzer), interfaced to a computer, allowed the recording of the direct impedance spectroscopy measurements.

Impedance spectroscopy measurements were carried out in a symmetry three-electrode cell in air at temperature, T, between 973 and 1273 K. The complex impedance measurements were made over the frequency range of 0.1-10⁶ Hz with a 10 mV AC signal amplitude at equilibrium potential and thermal.

Results and discussion

XRD patterns confirm that all the prepared samples are characterised by the orthorhombic perovskite-type structure, whose unit cell size diminishes with the increase of *x*. The SEM micrographs of the electrode/electrolyte interface showed that the uniform thickness of the cathode, as well as good contact between phases are achieved; the electrodes produced in this study are always 40-50 μm thick. In this way, it is measured that, under strictly controlled conditions (printing technique, temperature, etc), this is constant for all samples.

Under the experimental conditions employed at high temperatures (T>973K), the observed

complex impedance plot consists of a single arc due to the impedance at the electrode/electrolyte interfaces. In particular, complex impedance measurements of the pure LaMnO_3 or $\text{La}_x\text{Ca}_{1-x}\text{MnO}_3$ -electrodes typical produced suppressed single arcs. In fact the impedance arc was slightly depressed (at lower temperatures the high-frequency ends of the arcs intercepted the real axis at a 45° angle), suggesting that the interface impedance is expressed not only by a single RC parallel circuit but also by the small additional contribution of the Warburg type (diffusional) impedance^{11,21}.

The best fits resulted from the equivalent circuit $\text{LR}_1(\text{R}_2/\text{CW})$. The inductance (L) was attributed to high frequency artifacts arising from apparatus. The first resistors (R_1) corresponded to the resistance of electrolyte and the lead wires. The remaining components related to the electrode, where R_2 was the resistance of the primary arc, and the capacitance (C) and Warburg impedance (W) represented diffusion properties.

In accord with many other authors, in this paper as the first approximation, we assumed that the electrode interface impedance can be expressed by a simple $\text{R}_1(\text{R}_2\text{C})$ equivalent circuit^{18,22,23,24}, as shown in Figure 1.

For data analysis, non-linear least-squares fitting was performed using the eimvrt program. As many other authors have done, from the impedance arcs obtained by complex impedance measurements, we determined the electrode interface conductivity (σ_{el}) and apparent capacitance (C_{el}) by the equations $\sigma_{\text{el}}=1/\text{AR}_{\text{el}}$ and $\text{C}_{\text{el}}=\sigma_{\text{el}}/2\pi f_{\text{T}}$ respectively, where A is the apparent area of YSZ surface on which electrode was mounted, R_{el} is the electrode interface resistance obtained from the impedance arc, and f_{T} is the frequency corresponding the top of the impedance arc²⁵. The parameters extracted from the fit to the impedance data are listed in Table 1.

In this way the temperature dependencies of R_1 and R_2 were obtained; in particular, R_2 decreases continuously with increasing electrochemical cell temperatures. Instead the high frequency intercept (R_1) was independent of T, as expected given that R_1 is associated with ionic conduction in the YSZ electrolyte. In addition R_1 is invariant with also operation time, while R_2 progressively slowly increases to reach a steady value.

From this data, the R_1 components has been assigned to the YSZ electrolyte resistance (R_o). The R_2 component is indicative of being related to the oxygen reduction reaction (R_{el}). In Table 1 the resistance R_2 of $La_xCa_{1-x}MnO_3$ electrodes at different temperatures and compositions is reported. The cathodic activity of perovskite electrodes was monitored with cell operation by extracting the R_{el} values from the impedance spectra.

We can determine the activation energy (E_{el}) for cathode reactions from a plot of the natural log of the R_{el} components versus the reciprocal of the absolute temperature in Kelvin. According to the Arrhenius equations, a plot of the natural log of the R_{el} for the cathodic reaction at different temperatures versus the inverse of the temperature in Kelvin is a straight line with a slope equal to $-E_{el}/R$, where E_{el} is the temperature-depend phenomenological energy of activation and R is the gas constant²⁶. In the context of our analysis, Figure 2 shows the temperature dependence of R_2 (or R_{el}) for $La_xCa_{1-x}MnO_3$ electrodes, which yielded an activation energy (E_a) between ~ 1 eV ($x=0,5$ and $x=1$) and $\sim 2,3$ eV ($x=0,33$). This high activation energy of R_{el} is very similar to prior reports, where it was interpreted as a limiting reaction step involving both oxygen dissociation and adsorption. The capacitance (C) associated with the perovskite electrodes was independent of temperature²⁷. Figure 2 shows the activation energy E_a for pure alkaline earth metal-doped lanthanum manganite perovskite electrodes as a functions of composition.

Conclusion

The characteristics of alkaline earth metal-doped lanthanum manganite perovskite $La_xCa_{1-x}MnO_3$ ($0 < x < 1$)– Y_2O_3 -stabilized ZrO_2 (YSZ) electrodes were investigated by *ac* impedance spectroscopy. In particular, the impedance of an interface between $La_xCa_{1-x}MnO_3$ and YSZ has been analysed as a function of temperature (T) and composition (x) in air.

The electrocatalytic properties (E_{el}) of the air electrode manganites in solid oxide fuel cells were examined between $\sim 900K$ and $\sim 1273K$.

Electrochemical impedance spectroscopy is found to be useful for investigating perovskite

cathodes, although the data are not straight forward to interpret due to several overlapping process and the influence of parameters non related to the oxygen reduction process. For this reason, details of the reaction mechanisms as a function of composition, in the whole composition range, and O₂ pressure will be studied in future investigations.

References

1. M.Napoletano, J.M.Gallardo Amores, E.Magnone, G.Busca, M.Ferretti, *Physica C*, 1999, **319**, 229.
2. O.Yamamoto, Y.Takeda, R.Kanno, M.Noda, *Solid State Ionics* **22** (1987) 241.
3. Keikichi Nakamura, *Journal of Solid State Chemistry* **173**, 2 (2003) 299.
4. L.A.Tikhonova, A.A.Vecher, G.I.Smal, P.P.Zhuk, A.A.Tonayan, M.P. Gilevich, *Vestn. Belorus. Univ. Ser.*, 1988, 2 - 3, 13
5. I.G. Krogh Andersen, E. Krogh Andersen, P. Norby and E. Skou. *J. Solid State Chem.* **113** (1994) 320
6. M.Ferretti, E.Magnone, M.Napoletano, *Int. J. Modern Physics B*, 1999, **13**, 9&10, 979.
7. V. L. Joseph Joly, P. A. Joy and S. K. Date, *Journal of Magnetism and Magnetic Materials*, 2002, **247**, 3, 316-323.
8. N. N. Loshkareva, T. I. Arbuzova, I. B. Smolyak, N. I. Solin, S. V. Naumov, Yu. P. Sukhorukov, E. V. Mostovshchikova, N. A. Viglin, A. V. Korolyov, A. M. Balbashov M. Hennion, F. Moussa and G. Papavassiliou, *Journal of Magnetism and Magnetic Materials*, 2002, **242-245**, 2, 704-706.
9. T.Kenjo, M.Nishiya, *Solid State Ionics*, 1992, **57**, 295.
10. C.N.R.Rao, A.K.Cheetham, R.Mahest, *Chem. Mater.*, 1996, **8**, 2421
11. D.D. McDonald, M.C.H.McKubre, in: J.R McDonald (Ed.), *Impedance Spectroscopy*, Wiley, New York, 1987.
12. Hee Y.Lee, Seung M. Oh, *Solid State Ionics*, 1996, **90**, 133-140.
13. H.Yokokawa, N.Sakai, T.Kawada, M.Dokiya, *J. Electrochem. Soc.*, 1991, **139**, 9, 2719-2727

14. M.J.Jorgensen, S.Phimdahl, M.Mogensen, *Electrochimica Acta*, 1999, **44**, 4195.
15. Jae-Dong Kim, Goo-Dae Kim, Ji-Woong Moon, Yong_il Park, Weon-Hae Lee, Koichi Kobayashi, Masayuki Nagai, Chan-Eun Kim, *Solid State Ionics*, 2001, 143, 379.
16. T. Kawada, N. Sakai, H. Yokokawa and M. DokiyaM. MoriT. Iwata, *Solid State Ionics*, **40-41**, (1990) 402.
17. C.Bocca, G.Cerisola, E.Magnone, A Barbucci, *Int. J. Hydrog. Energy*, 1999, **24**, 699.
18. J. Van Herle, A.J.McEvoy and K.Ravindranathn Thampi, *Electrochimica Acta*, 1996, **41**, 9, 1447.
19. Xin Guo, Jürgen Fleig and Joachim Maier *Solid State Ionics*, **154-155** (2002) 563-569
20. A. Barbucci, R. Bozzo, G. Cerisola and P. Costamagna, *Electrochim. Acta* **47** (2002) 2183.
21. J.E.Bauerle, *J. Phys. Chem. Solids*, 1969, **30**, 2657.
22. J.Sasaki, J.Mizusaki, S.Yamauchi, K.Fueki, *Bull. Chem. Soc. Jpn.*, 1981, **54**, 1688.
23. K.Tsuneyoshi, K.Mori, A.Sawata, J.Mizusaki, H.Tagawa, *Solid State Ionics*, 1989, **35**, 263.
24. J.Q.Li, P.Xiao, *Journal of the European Ceramic Society* **21** (12001) 659.
25. J.Mizusaki, H.Tagawa, K.Tsuneyoshi, A.Sawata, *J.Electrochem. Soc.* **138**, 7, (1991) 1867.
26. Donald G.Truhlar, A.Kohen, *PNAS*, 2001, **98**, 3, 848.
27. J.T.S. Irvine, D.C.Sinclair, A.R.West, *Advanced Materials*, 1990, **2**, 132.

TABLE. 1. The resistance (R_2 in Ω) of $\text{La}_x\text{Ca}_{1-x}\text{MnO}_3$ electrodes at different temperatures and compositions.

Samples	x (La)	923 K	973 K	1023 K	1073 K	1123 K	1173 K	1223 K	1273 K
LCM25	0.25	3700	1130	307	81	61	27	16	13
LCM33	0.33	7080	3850	1100	229	102.5	27	8.85	2.72
LCM50	0.5	808	998	722	648	364	120	74	27
LCM53	0.53	4840	2500	1250	290	192	83	55	38
LCM55	0.55	4420	1208	330	63	47	25	13	5.46
LCM60	0.6	3640	893	621	275	137	45	37	26
LCM63	0.63	1690	1100	658	269	133	42.6	25	17
LCM67	0.67	1700	444	295	151	55	23	10	5.2
LCM75	0.75	1120	637	235	114	44	23	11	10
LMO	1	4210	1700	950	665	285	181	132	91

TABLE. 2. Activation energy E_a (eV) for pure alkaline earth metal-doped lanthanum manganite perovskite electrodes as a functions of composition.

Sample	LCM25	LCM33	LCM50	LCM53	LCM55	LCM60	LCM63	LCM67	LCM75	LMO
E_a (eV)	1.681	2.338	0.996	1.497	1.897	1.323	1.441	1.641	1.486	1.105

Figure captions

Fig. 1. (a) The equivalent electrical circuit model for pure alkaline earth metal-doped lanthanum manganite perovskite electrodes and (b) the equivalent circuit used for fitting the data.

Fig. 2. Activation energy E_a (eV) for pure alkaline earth metal-doped lanthanum manganite perovskite electrodes.

FIG. 1.

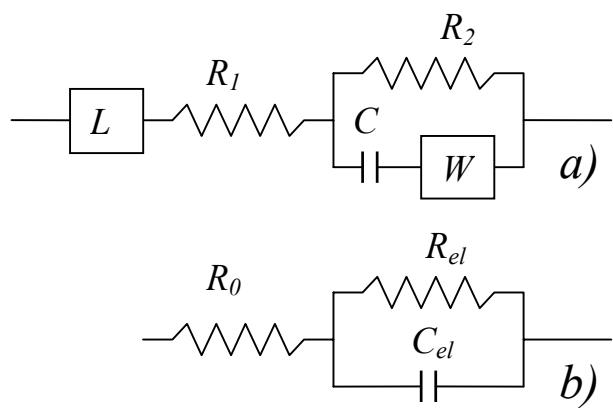


Fig. 2

